Clays and Clay Minerals, Vol. 39, No. 5, 540–550, 1991.

TRANSMISSION ELECTRON MICROSCOPE OBSERVATIONS OF ILLITE POLYTYPISM[1]

SUSAN M. BAXTER GRUBB, DONALD R. PEACOR, AND WEI-TEH JIANG

Department of Geological Sciences, The University of Michigan
Ann Arbor, Michigan 48109-1063

Abstract—Transmission electron microscopy (TEM), including selected area electron diffraction (SAED), has been used to identify polytypes in illite, phengite and muscovite from samples representing a wide range of diagenesis and low-temperature metamorphism. Samples include Gulf Coast sediments, sediments from the Salton Sea region, California, the Martinsburg Formation at Lehigh Gap, Pennsylvania, the Kalkberg Formation at Catskill, New York, Otago Schists from southern New Zealand, pelites from the Gaspé Peninsula in Quebec, Canada, shales and slates from Wales, sediments from the Barbados accretionary complex, and synthetic hydrothermal illite.

Samples from rocks of lowest grades, including those representing a range of sedimentary diagenesis, invariably give SAED patterns with few, complex non-00*l* reflections which are diffuse and ill-defined and that represent largely disordered stacking sequences. Corresponding XRD patterns are consistent with $1M_d$ polytypism. The term $1M_d$ is therefore retained for this material. Higher grade samples, including those in which slaty cleavage is developed, and detrital grains in low-grade sediments invariably give diffraction patterns of well-ordered 2- or 3-layer polytypes. Of all samples and localities studied, only one diffraction pattern, from a sample in the Gaspé sequence, was found to be predominantly $1M$. In none of the other sequences included in this study were any $1M$ or predominantly $1M$ electron diffraction patterns obtained for illite grains.

Where illite is in its original state of formation, it is consistently $1M_d$, whether it originates as a result of direct crystallization from solution or as a replacement of smectite. Where illite has apparently undergone subsequent change, presumably through dissolution and crystallization representing an Ostwald-step-rule-like change, it occurs as a well-ordered 2-layer (inferred to be $2M_1$) or, less commonly, a $3T$ polytype. On the basis of this limited survey, the state of polytypism appears to directly identify illite as either being in, or changed from, its initial state of formation.

Key Words—Illite, Polytypism, Transmission electron microscopy.

INTRODUCTION

The existence of a sequence of transformations between polytypes of aluminous dioctahedral micas from $1M_d$ through $1M$ to $2M_1$, occurring as a function of increasing grade of diagenesis-metamorphism, has been accepted for many years (e.g., Yoder and Eugster, 1955; Velde, 1965; Kisch, 1983; Mukhamet-Galeyev *et al.*, 1985). It has been suggested (Velde, 1965) that $1M$ and $1M_d$ polytypes are metastable and that $2M_1$ is the stable polytype of dioctahedral white micas; however, in sedimentary rocks $1M_d$ is the predominant form. Kisch (1983) suggested that the $1M$ to $2M_1$ transition is complete by the onset of greenschist-facies metamorphism.

Subsequent to the description of the six simple mica polytypes ($1M$, $2M_1$, $2M_2$, $2O$, $3T$, and $6H$) by Smith and Yoder (1956), much research has been devoted to the structural and chemical factors controlling polytypism. The effect of compositional variation on mica structure (and in turn polytypism) is documented by Güven (1971) and Abbott and Burnham (1988). Güven (1971) proposed that different polytypes result from the deviations of single mica layers from ideal $C2/m$ symmetry as a result of compositional variation, degree of Al^{3+}–Si^{4+} ordering, and distortions resulting from octahedral substitutions and vacancies combined with interlayer shift parallel to corrugations in the basal O planes of the tetrahedral layers. Abbott and Burnham (1988) explained the frequency of occurrence of the simple polytypes as a function of the amplitude of corrugations in the basal O surface, and tetrahedral rotation. As the proportion of octahedral Mg^{2+} increases (i.e., phengite component increases), the amplitude of basal corrugations decreases, as does the effect of those corrugations in determining polytype stability (Abbott and Burnham, 1988). Polytypes with long-period repeats have been attributed to growth along single screw dislocations on (001) of simple polytypes (Smith and Yoder, 1956; Baronnet, 1975; Pandey *et al.*, 1982).

Illite varies in composition from muscovite in that it has a smaller Al/Si ratio, and therefore a lower net negative charge and correspondingly smaller number of charge-balancing interlayer K^+ ions. In addition, most illite grains are less than 2 microns in size (Grim, 1968). Most mica-like materials that have been characterized as being $1M_d$ are illite rather than muscovite. However, such materials have compositions that approach that of muscovite with increasing grade of metamorphism. Increasing tetrahedral charge deficiency and K^+ con-

[1] Contribution No. 479 from the Mineralogical Laboratory, Department of Geological Sciences, The University of Michigan, Ann Arbor, Michigan 48109.

Copyright © 1991, The Clay Minerals Society

https://doi.org/10.1346/CCMN.1991.0390509 Published online by Cambridge University Press

tent, as well as decreasing octahedral charge and water content, is concomitant with the transformation to the $2M_1$ polytype (Kisch, 1983; Hunziker *et al.*, 1986; Lee *et al.*, 1986). Środoń *et al.* (1986) proposed the existence of two distinct illite compositions (having 0.55 and 1.00 K^+ per illite layer, respectively). These were hypothesized to combine and create averages ranging between the end members. Such a scheme differs substantially from that of the generally-accepted single solid solution series ranging between end members as a result of substitutions in sites of a single kind of structural unit. According to Środoń *et al.* (1986), the transition between the two types of illite is accomplished through a mechanism of dehydration of interlayer hydrated K^+ as it is fixed, rather than by neoformation. Środoń *et al.* (1986) also propose an increase in ordering of structure with increasing K^+ content.

Based on geological occurrences, Mukhamet-Galeyev *et al.*, (1985) inferred that the $2M_1$ polytype is stable, and that the transition from the $1M$ polytype should occur in a geologically reasonable time span at temperatures above 350°C. Their experiments demonstrated that the transition from $1M$ to $2M_1$ polytypes occurs via solution, with crystallization of $2M_1$ as the rate-limiting step. The results of their syntheses indicate that both $2M_1$ and $1M$ polytypes form directly from gel, but the rate of crystallization of $2M_1$ is much slower. As a result, there is much more $1M$ material after initial crystallization. Upon completion of recrystallization, the $1M$–$2M_1$ transition was said to have taken place, with the earlier-formed $2M_1$ crystals serving as nuclei. Velde (1965) produced $2M$ muscovite experimentally at lower temperatures (225°C, 4 Kb) than described by Mukhamet-Galeyev *et al.* (1985). Lee *et al.* (1985) have documented the transition from $1M_d$ illite in bedding orientation of shales of the Martinsburg Formation (Lehigh Gap, Pennsylvania) to 2-layer polytype illite in cleavage orientation of slates, via dissolution and crystallization.

In a strict sense, the changes in stacking sequence discussed in this paper do not relate to true polytypism. Polytypism requires, *sensu stricto,* that changes in stacking sequence are not accompanied by changes in composition, whereas the dioctahedral minerals described herein vary in composition from illite to muscovite and phengite with increase in grade of diagenesis/metamorphism. Nevertheless, we will use the term polytypism in reference to the changes in stacking sequence, as is traditional, but with the caveat that such usage is inexact.

Most studies of polytypism have relied on X-ray diffraction (XRD) to identify mica polytypes. Smith and Yoder (1955) described methods of identification of polytypes using powders and single crystal samples. These methods have subsequently been used by several others (e.g., Levinson, 1955; Velde and Hower, 1963; Reynolds, 1963; Velde, 1965; Maxwell and Hower, 1967; Karpova, 1969; Frey *et al.*, 1983; Bailey, 1984, 1988; Mukhamet-Galeyev *et al.*, 1985; Hunziker *et al.*, 1986; Inoue *et al.*, 1987, 1988; Austin *et al.*, 1989; DiMarco *et al.*, 1989). It has been shown that sample characteristics, such as grain size and interferences from nonclay sample components, have a significant effect on polytype determination by XRD (Hughes *et al.*, 1988; Austin *et al.*, 1989). Austin *et al.* (1989) note that the term $1M_d$ refers, *sensu stricto,* to the disordered polytype associated with the $1M$ ordered polytype, and that this term has frequently been misused in reference to disordered samples consisting of non-$1M$ polytypes or interlayered smectite. These errors are easily avoided with the TEM methods employed in this study because the polytype of individual illite grains is observed directly. Recent studies using TEM have demonstrated that phyllosilicates in sub-greenschist facies rocks are extremely heterogeneous (Lee *et al.*, 1985, 1986; Ahn and Peacor, 1986; Yau *et al.*, 1987a, 1987b, 1988). Polytypism varies not only between grains within a single sample, but also within individual grains.

One advantage of XRD methods is that they lead to determination of stacking sequences that are averages for heterogeneous material, and thus reflect the significant, dominant polytype. However, polytype determinations using such methods may include material from a variety of origins (e.g., detrital vs. authigenic) and do not directly characterize specific grains, or generations of grains, of illite. On the other hand, transmission electron microscopy is capable of direct characterization of polytypism in individual grains (e.g., Iijima and Buseck, 1978; Amouric *et al.*, 1981; Iijima and Zhu, 1982). More importantly, the origins of such grains can be determined through a variety of methods that include direct imaging of textural relations and determination of composition through high resolution energy dispersive X-ray analysis. Care must be taken to verify that the results from small specimen areas are representative of the average material.

Diffraction patterns and lattice-fringe images of illite, phengite, muscovite, and other micas have been obtained from a large number of localities and environments by several workers in the Mineralogical Laboratories of the University of Michigan. Although polytypism was documented, no attempt has been made to correlate the results. Therefore, we have reviewed the TEM data in order to determine trends in polytypism from as large a variety of environments as possible. We utilized results only from grains for which a nondetrital origin had been established.

METHODS AND MATERIALS

Microscopy and diffraction

All observations were made using ion-milled samples. Except for products of the hydrothermal experiments, all TEM samples were obtained from thin sec-

https://doi.org/10.1346/CCMN.1991.0390509 Published online by Cambridge University Press

tions, and thus original textural relations were retained. Detailed procedures are described in the separate papers cited. TEM observations were made using a JEOL 100-CX stem. A CM12 instrument was used for observations of samples from Wales, Barbados, Gaspé Peninsula, and some samples from the Gulf Coast. SAED patterns, textures in TEM images, lattice-fringe images, and EDS analyses were used for illite identification.

All of the SAED patterns from the studies cited were available. However, only those patterns were used for which c* was perpendicular to the electron beam and where non-00*l* reflections were present for which $k \neq 3n$. Polytypes can only be identified under these conditions. There are three 2-layer polytypes, $2O$, $2M_1$, and $2M_2$, and one 3-layer polytype ($3T$), dioctahedral micas commonly being $2M_1$. Although some polytypes were identified as $2M_1$, only the periodicity was determined in most samples. Therefore, the descriptions are simply characterized as 2-layer polytypes.

The principles involved in polytype identification by XRD and electron diffraction have the same basis. For dioctahedral micas, the contributions of octahedral cations and anions dominate the $k = 3n$ reflections (ions that repeat at an interval of b/3). The $k \neq 3n$ reflections are dominated by the contributions from tetrahedral cations and basal oxygens (ions that have interruptions or do not repeat at intervals b/3) (Bailey, 1988). Therefore, polytypes can be identified from the periodicity of the $k \neq 3n$ reflections, corresponding to the periodicity of rotations of the 2:1 layers. The 00*l* reflections give no polytype information owing to their insensitivity to variations in x and y coordinates of atoms within planes. For $1M_d$ material, reflections having $k \neq 3n$ are diffuse as a consequence of the lack of ordered periodicity in the rotation of basal O planes.

Samples

Dioctahedral, aluminous clay minerals from a variety of localities, geological ages, and environments were examined for this study. They have been described in detail in separate publications, and therefore will only be reviewed briefly below. It is important to note however, that most samples come from prograde sequences that cover a significant portion of the range of diagenesis and low-grade metamorphism, up to and including the greenschist facies. All samples have been well characterized using a variety of techniques.

RESULTS

Gulf Coast samples (Cretaceous–Tertiary)

Samples from four different wells that span the smectite to illite transition have been studied. Ahn and Peacor (1986) studied specimens from the same suite that had been used by Hower *et al.* (1976) from the Case Western Reserve University Gulf Coast 6 well. In addition, Freed and Peacor (1991) examined samples from wells in Brazoria and Hidalgo counties, Texas that had originally been studied by XRD by Freed (1981, 1982), and Freed and Peacor (1991) have studied samples from a well in DeWitt County, Texas. As part of this study, SAED patterns were only examined that were obtained from specimens that contained the maximum proportion of illite layers in mixed-layer I/S. As determined by XRD data, that corresponds to approximately 85% illite in R = 1 I/S. It is important to note that such material is not true illite in that it contains a significant proportion of smectite layers.

The illite-rich crystallites gave SAED patterns with well-defined 00*l* reflections that showed 10-Å periodicity (Figure 1). Such a sequence of 00*l* reflections is very different from those of typical smectite, for which only 001 is relatively intense, but very diffuse. The corresponding lattice-fringe images are relatively straight (as opposed to the wavy, anastomosing fringes of smectite) fringes with 10-Å spacing and only rare layer terminations. This is the phase interpreted by Ahn and Peacor (1986) to be the "illite" that formed by dissolution and crystallization of enclosing smectite.

The non-00*l* reflections (where $k \neq 3n$) of such material were diffuse, discontinuous and relatively weak (Figure 1). Those reflections were somewhat diffuse parallel to c*. Their existence does imply some local order, but spacings between the reflections in the direction of c* were random, with no indication of 10-Å periodicity or a multiple thereof. The diffraction pattern shown in Figure 1 is typical of all those obtained in the studies described below and identified as being $1M_d$. We therefore refer to it as corresponding to the $1M_d$ polytype.

A principal reason that the non-00*l* reflections were so weak is that, as shown by *hk*0 diffractions of equivalent material by Freed and Peacor (1991), turbostratic stacking causes the reflections to be distributed as spotted rings concentric with c*. The two-dimensional SAED pattern is a cross section through such rings, but including the central axis c*. The latter is thus fully represented by all layers in a given stack, but non-00*l* reflections are contributed to by only a relatively small fraction.

Martinsburg Formation (Ordovician)

Samples obtained at Lehigh Gap continuously span the mudstone-to-slate transition over a distance of approximately 100 m. Mudstones have defect-rich illite oriented preferentially parallel to bedding, whereas slates are dominated by well-crystallized illite in the cleavage orientation. The latter illite is derived by dissolution and crystallization from that in the shale (Wintsch, 1978; Lee *et al.*, 1985, 1986).

Illite in the lowest grade mudstone samples yielded SAED patterns that predominantly correspond to $1M_d$ illite (Figure 2), as described for Gulf Coast samples. Corresponding XRD patterns were consistent with this

https://doi.org/10.1346/CCMN.1991.0390509 Published online by Cambridge University Press

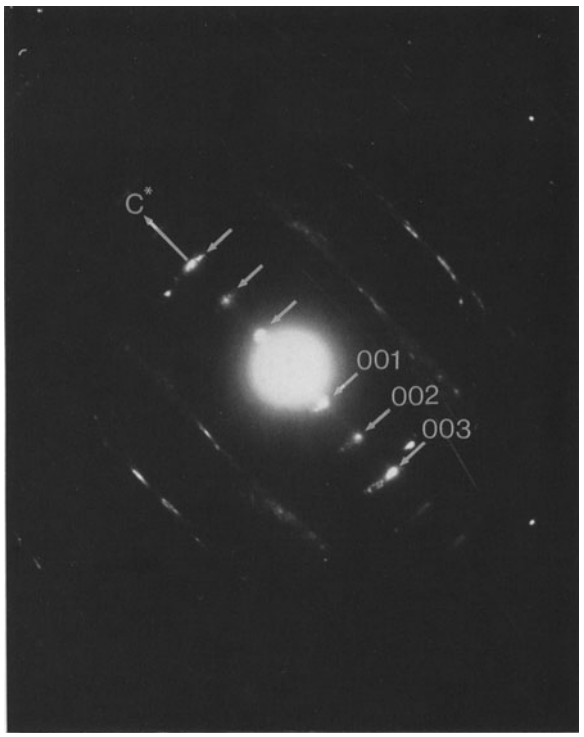


Figure 1. Selected area diffraction pattern of $1M_d$ Gulf Coast illite formed by replacement of smectite. Streaking of non-00*l* reflections (where $k \neq 3n$) reflects a largely-disordered stacking sequence. Irregular reflections superimposed on these streaks represent local ordering. Large arrows indicate 00*l* reflections (photo by Jung Ho Ahn).

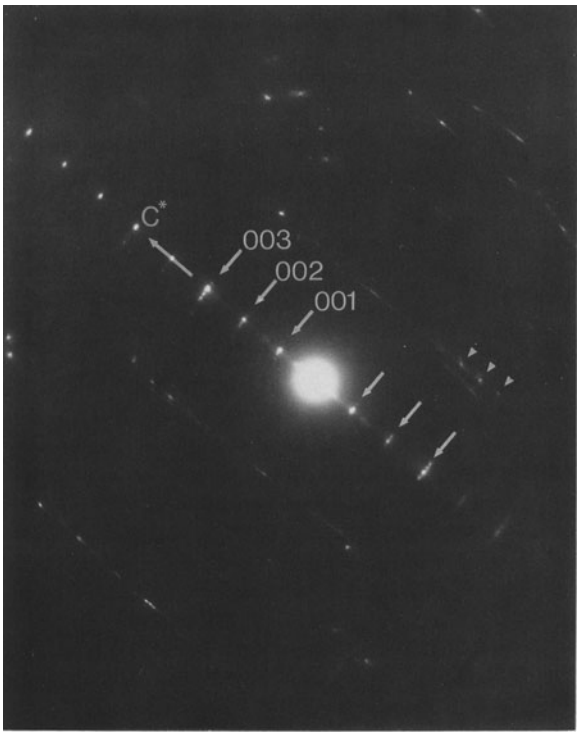


Figure 2. Selected area diffraction pattern of illite from the Martinsburg shale. Small arrows indicate reflections due to locally-ordered stacking with superimposed streaking indicative of disordered stacking. Large arrows indicate 00*l* reflections (photo by Jung Hoo Lee).

phase being true illite, rather than mixed-layer I/S. Shale samples transitional between mudstone and slate showed an increase in frequency of occurrence of the 2-layer polytype and a decrease in $1M_d$ that parallels the shift in predominance from bedding-parallel to cleavage-parallel illite grains. SAED patterns of illite in slate samples that have fully-developed slaty cleavage had sharp reflections with no streaking, with well-defined 20-Å periodicity (Figure 3A). Dynamical diffraction relations gave rise to 20-Å periodicity in 00*l* reflections, whereas only 10-Å periodicity was observed for the same grains when non-00*l* reflections were absent from the diffraction patterns. The 20-Å periodicity would, of course, not be observed in XRD patterns. Lattice-fringe images derived from the selected area diffraction patterns showed typical 20-Å periodicity through alternating contrast of lattice fringes (Figure 3B).

Salton Sea sediments (Plio-Pleistocene)

These samples span the range from smectite-rich sediments that have been little affected by diagenesis through greenschist-facies hornfels (Helgeson, 1968). Two types of illite occurred as described by Yau *et al.* (1987a): (1) packets of layers intergrown with and derived from smectite, as in Gulf Coast sediments, and (2) subhedral, hexagonal crystals filling pore space and derived by crystallization from solution. Samples that have been studied came from the No. 2 Imperial Irrigation District well (IID 2), the Elmore No. 1 well (Yau *et al.*, 1987a), and the Salton Sea Scientific Drilling Project/California State 2-14 well (CS 2-14).

Both kinds of illite gave SAED patterns equivalent to those described above for Gulf Coast illite-rich I/S. These patterns displayed non-00*l* reflections that were diffuse, irregular in shape, and showed no measurable periodicity along c* (Figure 4). The hexagonal crystallites occupying pore space that were derived through direct crystallization from hydrothermal fluids were characterized as true illite; i.e., XRD patterns showed that they contained virtually no expandable component.

South Island metasediments, New Zealand (Carboniferous–Triassic)

Samples were collected along a near-shore sequence south of Dunedin, extending from south of Nugget Point northward to Brighton. This is a nearly continuous prograde sequence ranging from Triassic zeolite

https://doi.org/10.1346/CCMN.1991.0390509 Published online by Cambridge University Press

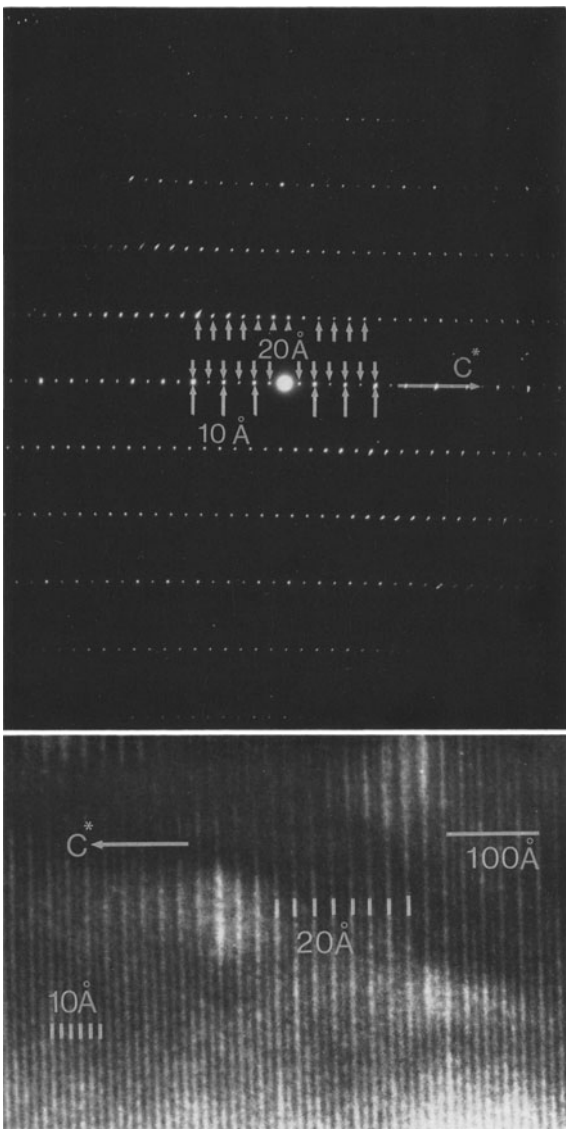


Figure 3. A. Selected area diffraction pattern of 2-layer illite polytype from the Martinsburg slate. Long arrows indicate 00*l* reflections. Short arrows denote sharp 20-Å reflections showing periodicity of the polytype. B. Lattice-fringe image of 2-layer polytype from the Martinsburg Formation. The 2-layer periodicity of the polytype is indicated by alternating contrast of the 001 lattice fringes (photos by Jung Hoo Lee).

facies volcanogenic sediments through biotite grade (Haast Schist) metasediments, as summarized by McKellar (1966). TEM data obtained for samples at the lowest (Nugget Point) and highest (Brighton) grade samples were described by Ahn *et al.* (1988) and Ahn and Peacor (1987), respectively.

Illite from pelites within the zeolite facies gave SAED patterns reflecting $1M_d$ stacking sequences, and corresponding lattice-fringe images displayed no superperiodicities, as was always observed for corresponding $1M_d$ SAED patterns. Samples of pelites from grades greater than that of the zeolite facies through those of biotite grade all showed 2-layer polytypism or occasional $3T$ polytypism, and they yielded lattice-fringe images having contrast with 2-layer or 3-layer periodicity. Such samples ranged from those with poorly-developed cleavage through phyllites.

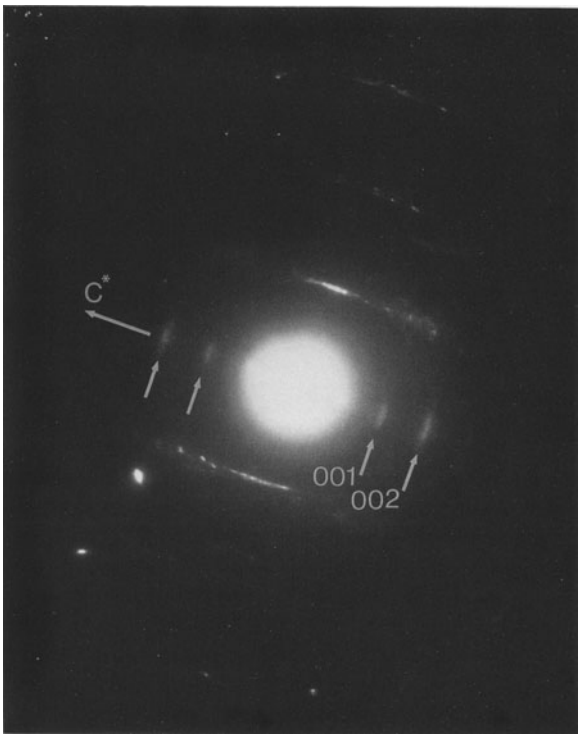


Figure 4. Selected area diffraction pattern of locally-ordered $1M_d$ hydrothermal illite from the Salton Sea sediments (photo by Yu-Chyi Yau).

Synthetic hydrothermal samples

Hexagonal crystals of illite were synthesized by direct crystallization from solution with starting materials consisting of illite from Fithian, Illinois and mixtures of smectite and basalt (Yau *et al.*, 1987b).

In those experiments for which changes in starting materials occurred, subhedral-to-euhedral illite and berthierine crystallites were observed. These were similar in appearance to the hydrothermal illite crystallites described by Yau *et al.* (1987a) as having formed through dissolution of detrital smectite and crystallization of illite in pore spaces. SAED patterns of the illite showed that it is $1M_d$, with patterns identical to those described above. One diffraction pattern corresponded to that of a 2-layer polytype. It could have originated either through dissolution of original metastable $1M_d$ illite or through direct crystallization of its components as the observed 2-layer polytype.

https://doi.org/10.1346/CCMN.1991.0390509 Published online by Cambridge University Press

Gaspé Peninsula samples (Ordovician)

Shale samples were studied that come from a prograde sequence for which illite crystallinity varies from approximately 0.6 to 0.2° Δ 2θ (CuKα radiation) (Jiang and Peacor, 1990). The majority of diffraction patterns obtained for illite grains in the lowest grade samples corresponded to $1M_d$ stacking sequences. Those samples gave XRD patterns with very broad illite reflections (crystallinity indices of approximately 0.6° Δ 2θ), and contained expandable trioctahedral phyllosilicates, including corrensite. SAED patterns showed that 2-layer polytypes were dominant in the higher grade rocks that displayed cleavage, had illite crystallinity indices as small as 0.25° Δ 2θ, and contained chlorite as the trioctahedral phyllosilicate. The larger, more defect-free grains of 2-layer polytypes were inferred to have developed through dissolution of low-grade illite and crystallization at higher grades (Jiang and Peacor, 1990). One grain from a rock of intermediate grade gave an SAED pattern of the $1M$ polytype. However, there was faint streaking of the non-00l reflections, indicating some disorder in the stacking sequence. This grain is the only one that we have observed that consists of the $1M$ polytype. Unfortunately, no chemical data were obtained for it, and it is possible that it was biotite, as the common $1M$ polytype of biotite has been commonly observed in the lowest grade samples.

Kalkberg Formation (Devonian)

Shaly limestone samples were studied that came from a single continuous shaly limestone bed. Folding into an anticline gave rise to virtually complete pressure-dissolution of carbonates on one limb of an anticline, producing a shale (Kreutzberger and Peacor, 1988). Illite both from the limestone unaffected by pressure solution, and the shale produced by carbonate dissolution, gave SAED patterns displaying well-defined 2-layer polytypism. Packets of illite were observed to be significantly larger as a result of the pressure solution process.

Welsh sedimentary basin (Ordovician)

Jiang *et al.* (1990) studied a mudstone that has been altered, presumably by fluids from a nearby fault, showing partial alteration of a 2-layer polytype of illite (that formed under anchizonal conditions) to mixed-layer I/S. Basin sediments show a continuous change in illite crystallinity indices that indicate a range in grade from late diagenesis through epizonal conditions (Merriman and Roberts, 1985). Merriman *et al.* (1990) showed that the changes in crystallinity were caused by progressive increase in the thickness of illite packets through dissolution and crystallization mechanisms. All illite was observed to consist of well-ordered 2- or 3-layer polytypes.

Barbados accretionary wedge (Cenozoic)

Buatier *et al.* (1991) have studied smectite-rich sediments in the Barbados accretionary wedge that are approximately 2000 feet in thickness. The deepest samples contained crystallites of neoformed illite (or illite-rich I/S, as in Gulf Coast pelites) within a matrix of smectite. The crystallites consist of $1M_d$ illite (or illite-rich I/S).

*"Illite" identified as being 1*M *by XRD*

Because the observation of only a single grain of $1M$ illite in samples for which a complete sequence from $1M_d$ to 2-layer polytypes is at variance with many observations (e.g., Levinson, 1955; Velde and Hower, 1963; Karpova, 1969; Eberl *et al.*, 1987; Inoue *et al.*, 1987, 1988; Austin *et al.*, 1989), two samples for which XRD data had indicated the presence of $1M$ illite were studied by TEM.

One sample, provided by R. E. Hughes of the Illinois Geological Survey, was a greenish mineral separate from the St. Peter sandstone in Illinois. It was characterized as containing $1M$ illite using powder XRD techniques (Hughes, personal communication). TEM data showed the presence of only the $1M$ polytype. AEM analyses (normalized to a tetrahedral + octahedral cation content of 6.062, i.e., with a small trioctahedral component for charge balance) gave rise to the formula: $(K_{0.73}Na_{0.05}Ca_{0.02})$ $(Al_{0.93}Mg_{0.55}Fe^{3+}_{0.50}$-$Fe^{2+}_{0.08})$ $(Si_{3.64}Al_{0.36})O_{10}(OH)_2$. It was rich in Fe^{3+}, intermediate in composition to celadonite, glauconite and illite, and was therefore not typical of the Al-rich illite, phengite, and muscovite that were the source of data in all other studies described here. These observations are consistent with the $1M$ polytype being dominant in celadonite-rich micas (Odom, 1984).

A second sample was provided by J. R. Walker. It was part of a study of variation in illite and chlorite from the Borchard A-2 well, Imperial Valley, California (Walker and Thompson, 1990) and was a mounted XRD sample that had originally led to identification of $1M$ illite. The powder was used in the preparation of an ion-milled sample. Grains of this clay mineral separate were exceedingly small (a few tens-of-Ångstroms in thickness), and gave rise to ill-defined $1M_d$ and $2M$ diffraction patterns. No $1M$ illite was observed. The $2M$ illite was interpreted to be detrital material.

Detrital dioctahedral 2:1 phyllosilicates

In many of the studies cited above, detrital grains of "white mica" were commonly observed. Such grains generally have compositions approaching that of muscovite (phengite) and consist of large, angular grains. Where their polytype has been determined, it has inevitably been observed to be a 2-layer polytype. Indeed, 2-layer polytypism can be taken as definitive evidence for the detrital origin of grains of dioctahe-

https://doi.org/10.1346/CCMN.1991.0390509 Published online by Cambridge University Press

Table 1. Summary of transmission electron microscopic observations of illite polytypism.

Location	Mode of origin	Polytypic state
Gulf Coast	1. replacement of smectite	$1M_d$
	2. detrital	2-layer
Martinsburg Fm.	1. replacement of smectite (shale)	$1M_d$
	2. dissolution/crystallization of illite/smectite from shale samples (slate)	2-layer
	3. detrital	2-layer
Salton Sea	1. replacement of smectite	$1M_d$
	2. hydrothermal product of smectite and illite	2-layer
	3. detrital	2-layer
New Zealand	1. zeolite facies dissolution of tuffaceous material followed by crystallization	$1M_d$
	2. regionally metamorphosed prehnite-pumpellyite through greenschist facies	2- and 3-layer
Hydrothermal	1. dissolution/crystallization	$1M_d$
Gaspé Peninsula	1. zone of diagenesis	$1M_d$
	2. lowest grade of metamorphism tectonic stress-induced transformation of smectite to illite	
	a) illite crystallinity ~ 0.65	$1M_d$
	b) illite crystallinity ~ 0.35	$1M_d$, $1M$(?) 2- and 3-layer
	c) illite crystallinity ~ 0.25 (° $\Delta 2\theta$, CuKα radiation)	2- and 3-layer
Kalkberg Fm.	1. pressure solution and localized dissolution/crystallization of regionally metamorphosed limestone	2-layer
Barbados Accretionary Wedge	1. illite as a replacement of smectite	$1M_d$
Welsh Pelites	1. tectonically-induced recrystallization of illite	2- and 3-layer

dral, aluminous 2:1 phyllosilicates occurring in low grade pelites.

DISCUSSION

The occurrence of the illites studied is summarized in Table 1. Illite, inferred to be in its original state of formation, was found in Gulf Coast samples, zeolite-facies samples from the Hokonui Hills, New Zealand, cleavage-free shales from the Martinsburg Formation, lower grade shales of the Gaspé Peninsula sequence, hydrothermally-synthesized samples, pelites of the Barbados accretionary wedge, and Salton Sea area sediments. Such illite occurred in three different modes: (1) as a product of direct crystallization from solution in open pore space, e.g., sediments of the Salton Sea Geothermal Field, (2) as packets of layers forming crystallites within a matrix of smectite, as in Gulf Coast and Barbados shales, and (3) as intergrown packets of layers in the cleavage-free shales that constitute the lowest grade rocks within a progressive prograde sequence, for which tectonically-induced cleavage occurs in higher grade rocks. Examples are the Martinsburg Formation, Welsh basin, New Zealand, and the Gaspé Peninsula.

With the exception of detrital material, the illite in such rocks gave rise to SAED patterns having the same characteristics. The 00*l* reflections resembled those of well-ordered polytypes except that reflections were somewhat broader with some diffuseness parallel to c*. Non-00*l* reflectins with $k \neq 3n$ were weak, very diffuse and broad, had irregular shapes, and exhibited no periodicity parallel to c*; indeed, very few such reflections were observed. A true $1M_d$ mica with absolutely no tendency for local order would give rise to non-00*l* reflections ($k \neq 3n$) consisting, theoretically, of continuous streaks parallel to c*. We have never observed such SAED pattens. XRD patterns of such material lack characteristic $k \neq 3n$ reflections. Our samples covered the range of illites for which the $1M_d$ polytype has been shown to exist through XRD studies. Because the irregular non-00*l* reflections of SAED patterns were so weak and ill-defined, we infer that they are characteristic of illites identified by XRD as $1M_d$ illite, and we therefore refer to that illite as being $1M_d$. Given the results for so many illite samples from low grade sequences that have not been subject to recrystallization, we conclude that illite that is in its initial state of formation has the same $1M_d$ stacking sequence.

On the other hand, 2- or 3-layer polytypes were observed for illite having (001) oriented preferentially parallel to the cleavage direction in slates of the Martinsburg formation, higher grade samples from the Gaspé sequence, samples from grades higher than that of the zeolite facies in New Zealand, shales and slates of the Welsh basin, all samples from the Kalkberg Formation, and, as observed in most localities, all detrital grains. SAED patterns showed relatively sharp non-00*l* reflections that defined a 20- or 30-Å periodicity

https://doi.org/10.1346/CCMN.1991.0390509 Published online by Cambridge University Press

parallel to c*. Only slight streaking was observed in some cases (Figure 3A), with corresponding periodicity in the contrast of lattice-fringe images (Figure 3B).

All of the samples which contain 2- or 3-layer polytypes occurred in rocks that have been subjected to tectonic stress, as shown, in part, by the progressive development of cleavage and deformation on a regional basis. In the case of the shale-to-slate transition, Lee *et al.* (1986) showed that the illite in the cleavage orientation was derived by dissolution of precursor illite and crystallization in the new preferred orientation. The sequence involves an increase in packet size as well as degree of preferred orientation, a decrease in proportion of defects, and a change in composition toward that of end-member muscovite or phengite. Such dissolution and crystallization processes are likewise implied by equivalent observations of samples from the other sequences. The 2- and 3-layer polytypes are thus inferred to have formed subsequent to, and at the expense of, $1M_d$ illite.

*Occurrence of the 1*M *polytype*

A curious result of this study is that only one crystallite of the $1M$ polytype was observed. Even in that sample streaking indicated stacking disorder. The mineral may have been biotite, which we commonly observe to give rise to disorder in stacking sequences and streaking in SAED patterns. The $1M$ polytype was not even observed as small proportions of 2-layer stacking sequences, for which reflections in SAED patterns were inevitably sharp, with a minimum of diffuseness. Yoder and Eugster (1955), Velde (1965), Kisch (1983), Mukhamet-Galeyev *et al.* (1985), and others have noted that there is a complete sequence of polytypes in dioctahedral white micas, from $1M_d$ to $1M$ to the stable $2M_1$ polytype. Although the results of this survey are consistent with the direction of changes in this sequence, with the $1M_d$ and $2M_1$ polytypes representing the beginning and ending states, our observation of only one example of the $1M$ polytype is, at first sight, puzzling.

Several studies for which polytypes were identified using XRD concur with our observations. Reynolds (1963) found no $1M$ illite in his survey of illite polytypism in Proterozoic carbonates. Hunziker *et al.* (1986) studied the illite-to-muscovite transition in samples from the Swiss Alps and found that all samples consisted either of $1M_d$ or $2M_1$ polytypes. Maxwell and Hower (1967) listed only a few instances of $1M$ illite, which they described as "questionable," in their study of illite polytypism in the Precambrian Belt Series.

On the other hand, $1M$ illite has been identified by XRD in many other natural samples. Levinson (1955) described a XRD powder pattern of $1M$ illite from the St. Austell china clay deposits, Cornwall. Velde and Hower (1963) also documented rare occurrences of $1M$ illite. Eberl *et al.* (1987) reported $1M$ illite in sericite from the Silverton caldera, Colorado. The material was determined by XRD to be mixed-layer I/S. Karpova (1969), Inoue *et al.* (1987, 1988), and Austin *et al.* (1989) have also identified $1M$ illite. Lonker and Fitz Gerald (1990) have recently observed $1M_d$, $1M$, and $2M$ illite in hydrothermally-altered siliceous volcanics and pyroclastics from the Broadlands-Ohaaki geothermal system, New Zealand. They showed that the 2-layer polytype of illite can be produced directly from $1M_d$ illite, although the $1M$ polytype occurred locally. Most importantly, Walker and Thompson (1990) have observed a complete sequence from $1M_d$ to $1M$ to $2M_1$ illite in sediments of the Salton Sea geothermal field, although our TEM results on one of their specimens cast some doubt on the existence of the $1M$ polytype.

Mechanisms for transition between polytypes

As a consequence of the structural differences between polytypes, a solid state transition is not a viable mechanism for transformation from one stacking sequence to another. Entire layers must be shifted relative to one another at low temperatures in a relatively stress-free environment. The major rearrangements of atoms can readily occur through dissolution and crystallization, however (Mukhamet-Galeyev *et al.*, 1985). The need for such a mechanism is further indicated by the changes in composition that accompany transformations from true illite to near-end member muscovite (increasing K^+ and $^{[4]}Al^{3+}$). Solid-state diffusion and interchange of ions, especially of Si and Al, do not occur in geologically reasonable times in the environments in question (Ahn and Peacor, 1986). Dissolution and crystallization are a step-like mechanism, whereas solid-state transitions would be continuous and gradual. Observation only of the $1M_d$ and 2-layer polytypes is consistent only with the former kinds of processes. The lack of continuous variation in orientations of illite grains in the Martinsburg Formation also implies that illite grains oriented with their basal planes parallel to cleavage formed by dissolution and crystallization at the expense of grains oriented parallel to bedding. This is opposed to a continuous restructuring transition as suggested by Hunziker *et al.* (1986).

According to the Ostwald step rule, the first phases to form by reaction of unstable phases are not necessarily the most stable form (viz., $2M_1$), but are metastable phases that may be disordered ($1M_d$). They are phases whose total free energy is less than that of precursor materials, but greater than that of the thermodynamically stable phases. Crystallization at low temperatures tends to give rise to heterogeneous, disordered, metastable phases. With time such metastable materials tend toward simple, more homogeneous states. However, the rate and path of subsequent changes toward a final stable equilibrium state are kinetically

https://doi.org/10.1346/CCMN.1991.0390509 Published online by Cambridge University Press

controlled, with crystallization of $2M_1$ illite being the rate-limiting step (Mukhamet-Galeyev *et al.,* 1985; Inoue *et al.,* 1988; Morse and Casey, 1988). Attempts to correlate the polytypic state of illite directly and quantitatively with pressure and temperature are therefore meaningless. Such correlations must be based on transformations between phases in states of stable equilibrium. On the other hand, the polytype of illite certainly is a measure of reaction progress, even though it cannot be directly correlated with absolute temperature.

The observation that the $1M_d$ polytype is ubiquitously observed for illite in its initial state of formation, derived either directly from solution in pore space, or through dissolution of precursor smectite and crystallization within a matrix of smectite, is thus consistent with Ostwald-step-rule relations. Such illite generally forms during diagenesis at very low temperatures, and in a tectonic stress-free environment. Tectonic stress, the presence of fluids, and higher temperatures subsequently cause dissolution of $1M_d$ illite. A "step" occurs, with 2-layer illite forming that, in conjunction with coexisting phases, constitutes a system at, or very near that, of a system at equilibrium. Metastability of phases forming at low temperatures, discontinuous (episodic) changes, and transitions occurring through dissolution and crystallization are therefore all self-consistent relations.

*Formation of 1*M *illite*

The lack of frequent observations of $1M$ illite by TEM in the samples of this study is curious because complete sequences inclusive of $1M_d$ and 2-layer polytypes are represented in the Martinsburg, New Zealand, Salton Sea, and Gaspé samples, and because the $1M$ polytype has been observed by XRD in intermediate samples of other studies. This is of particular concern with respect to the Salton Sea sequence, for which Walker and Thompson (1990) have independently observed the $1M$ polytype by XRD in intermediate samples. There are several explanations for this apparent inconsistency: (1) The TEM observations are based on a very small number of samples obtained from extensive sediment sequences. Especially if the $1M$ polytype is represented in a narrow range of samples, it is possible that they simply were not sampled in this study. (2) Trioctahedral micas and Fe^{3+}-rich dioctahedra, celadonitic and glauconitic micas commonly occur as the $1M$ polytype. The sample from the St. Peter sandstone described above, and celadonite from zeolite-grade volcanic sediments of New Zealand (Baxter and Peacor, unpublished data) are typical. Because XRD studies of polytypism generally did not include chemical data, it is possible that some reports of $1M$ illite actually corresponded to clay minerals with significant celadonite or glauconite components (e.g., Karpova, 1969). (3) The crystal chemical basis for polytypism is still incompletely understood, and it is possible that trace amounts of some cation, or some related factor, may result in the occurrence of the $1M$ polytype in selected cases. It is important to recall that the "polytype" transitions described in this paper did not occur between phases with identical compositions. (4) It has been shown that ambiguity exists in the determination of polytypic state (particularly $1M_d$ and $1M$) by XRD as a result of certain sample characteristics, sample preparation techniques, or misinterpretation of XRD patterns (Austin *et al.,* 1989). The Imperial Valley sample described here is apparently an example.

The most likely explanation, however, lies in the apparent very large difference in conditions for formation of $1M_d$ and 2-layer polytypes. Where conditions (P,T, fluid composition, water/rock ratio) vary continuously, then the Ostwald step rule predicts a series of transitions toward the system of lowest free energy. Where conditions vary discontinuously, as in tectonically-related episodic changes in low grade sediments, the step toward the final low energy state may be significantly larger, thus bypassing the $1M$ polytype. The samples of this study are all consistent with such an explanation.

Nevertheless, the observation of only a single grain of $1M$ illite in this study, and the lack of observation of the $1M$ polytype by XRD in intermediate samples of some other studies (e.g., Reynolds 1963; Maxwell and Hower, 1967; Hunziker *et al.,* 1986) is strong evidence for the occurrence of the $1M$ polytype only under relatively specialized conditions. Further TEM studies should be carried out on closely spaced samples for which XRD data indicate the presence of $1M$ illite in order to further define those relations.

ACKNOWLEDGMENTS

We thank J. H. Ahn, Y.-C. (Yau) Tsung, J. H. Lee, L. Donaghe, M. Kreutzberger, R. L. Freed, and M. D. Buatier for samples and TEM images. D. S. Coombs contributed some of the New Zealand samples. We are grateful to R. F. Hughes for providing clay mineral separates from the St. Peter sandstone, and J. Walker for an XRD sample from the Imperial Valley, California. We thank Y-H. Shau for his advice and help in the preparation of figures and S. Grubb for proofreading the manuscript.

The transmission electron microscopes used in this study were acquired under grants DMR-77-09634 and EAR-87-08276 from the National Science Foundation. This work was supported by National Science Foundation grants EAR-86-04170, EAR-831326, and EAR-88-17080 to D. R. Peacor.

REFERENCES

Abbott, R. N., Jr. and Burnham, C. W. (1988) Polytypism in micas: A polyhedral approach to energy calculations: *Amer. Mineral.* **73,** 105–118.

https://doi.org/10.1346/CCMN.1991.0390509 Published online by Cambridge University Press

Ahn, J. H. and Peacor, D. R. (1986) Transmission and analytical electron microscopy of the smectite-to-illite transition: *Clays & Clay Minerals* **34,** 165–179.

Ahn, J. H. and Peacor, D. R. (1987) Kaolinitization of biotite: TEM data and implications for an alteration mechanism: *Amer. Mineral.* **72,** 353–356.

Ahn, J. H., Peacor, D. R., and Coombs, D. S. (1988) Formation mechanisms of illite, chlorite and mixed-layer illite-chlorite in Triassic volcanogenic sediments from the Southland Syncline, New Zealand: *Contrib. Mineral. Petrol.* **99,** 82–89.

Amouric, M., Mercuriot, G., and Baronnet, A. (1981) On computer HRTEM images of perfect mica polytypes: *Bull. Mineral.* **104,** 298–313.

Austin, G. S., Glass, H. D., and Hughes, R. E. (1989) Resolution of the polytype structure of some illitic clay minerals that appear to be 1*Md*: *Clays & Clay Minerals* **37,** 128–134.

Bailey, S. W. (1984) Classification and structures of the micas: in *Micas, Reviews in Mineralogy, Vol. 13,* S. W. Bailey, ed., Mineralogical Society of America, Washington, D.C., 1–36.

Bailey, S. W. (1988) X-ray diffraction identification of the polytypes of mica, serpentine, and chlorite: *Clays & Clay Minerals* **36,** 193–213.

Baronnet, A. (1975) Growth spirals and complex polytypism in micas. I. Polytypic structure generation: *Acta Cryst.* **A31,** 345–355.

Buatier, M. D., Peacor, D. R., and O'Neil, J. R. (1991) Origin and evolution of clays in the sediments of the Barbados accretionary wedge (site 671B, Leg 110): *Eos, Trans. Am. Geophys. Union, suppl.* **72,** p. 269.

DiMarco, M. J., Ferrell, R. E., Jr., and Lowe, D. E. (1989) Polytypes of 2:1 dioctahedral micas in silicified volcanoclastic sandstones, Warrawoona Group, Pilbara Block, Western Australia: *Amer. Jour. Sci.* **289,** 649–660.

Eberl, D. E., Środoń, J., Lee, M., Nadeau, P. H., and Northrop, H. R. (1987) Sericite from the Silverton Caldera, Colorado: Correlation among structure, composition, origin and particle thickness: *Amer. Mineral.* **72,** 914–934.

Freed, R. L. (1981) Shale mineralogy and burial diagenesis of Frio and Vicksburg formations in two geopressured wells, McAllen Ranch area, Hidalgo County, Texas: *Gulf Coast Assoc. Geol. Soc. Trans.* **31,** 289–293.

Freed, R. L. (1982) Clay mineralogy and depositional history of the Frio Formation in two geopressured wells, Brazoria County, Texas: *Gulf Coast Assoc. Geol. Soc. Trans.* **32,** 459–463.

Freed, R. L. and Peacor, D. R. (1991) Diagenesis and the formation of authigenic illite-rich I/S crystals in Gulf Coast Shales: TEM study of clay separates: *J. Sediment. Petrol.* (in press).

Frey, M., Hunziker, J. C., Jager, E., and Stern, W. B. (1983) Regional distribution of white K-mica polymorphs and their phengite content in the central Alps: *Contrib. Mineral. Petrol.* **83,** 185–197.

Grim, R. E. (1968) Illite minerals: in *Clay Mineralogy,* 2nd ed. International Series in Earth and Planetary Sciences, McGraw-Hill, New York, 92–99.

Güven, N. (1971) Structural factors controlling stacking sequences in dioctahedral micas: *Clays & Clay Minerals* **19,** 159–165.

Helgeson, H. C. (1968) Geologic and thermodynamic characteristics of the Salton Sea geothermal system: *Amer. Jour. Sci.* **266,** 129–166.

Hower, J., Eslinger, E. V., Hower, M. E., and Perry, E. A. (1976) Mechanism of burial metamorphism of argillaceous sediments: 1. Mineralogical and chemical evidence: *Geol. Soc. Amer. Bull.* **87,** 725–737.

Hughes, R. E., Moore, D. M., Austin, G. S., and Glass, H. D. (1988) Further studies on the origin, identification, and quantification of illite polytypes: in *Program and abstracts, 25th Annual Meeting, The Clay Minerals Society, Grand Rapids, Michigan,* p. 49.

Hunziker, J. C., Frey, M., Dallmeyer, R. D., Freidrichsen, H., Flemig, W., Hochstrasser, K., Ruggwiler, P., and Schwander, H. (1986) The evolution of illite to muscovite: Mineralogical and isotopic data from the Glarus Alps, Switzerland: *Contrib. Mineral. Petrol.* **92,** 157–180.

Iijima, S. and Buseck, P. R. (1978) Experimental study of disordered mica structures by high-resolution electron microscopy: *Acta Cryst.* **A34,** 709–719.

Iijima, S. and Zhu, J. (1982) Electron microscopy of a muscovite-biotite interface: *Amer. Mineral.* **67,** 1195–1205.

Inoue, A., Kohyama, N., Kitagawa, R., and Watanabe, T. (1987) Chemical and morphological evidence for the conversion of smectite to illite: *Clays & Clay Minerals* **35,** 111–120.

Inoue, A., Velde, B., Meunier, A., and Touchard, G. (1988) Mechanism of illite formation during smectite-to-illite conversion in a hydrothermal system: *Amer. Mineral.* **73,** 1325–1334.

Jiang, W.-T. and Peacor, D. R. (1990) Parallel diagenesis/metamorphism of dioctahedral illite and trioctahedral chloritic minerals in the pelitic rocks of the Gaspe Peninsula, Quebec: in *Program and abstracts, 1990 Annual Meeting, Geol. Soc. of Amer., Dallas, Texas,* A258–259.

Jiang, W.-T., Peacor, D. R., Merriman, R. J., and Roberts, B. (1990) Transmission and analytical electron microscopic study of mixed-layer illite/smectite formed as an apparent replacement product of diagenetic illite: *Clays & Clay Minerals* **38,** 449–468.

Karpova, G. V. (1969) Clay mineral post-sedimentary ranks in terrigenous rocks: *Sedimentology* **13,** 5–20.

Kisch, H. J. (1983) Mineralogy and petrology of burial diagenesis (burial metamorphism) and incipient metamorphism in clastic rocks: in *Diagenesis in Sediments and Sedimentary Rocks, 2,* G. Larson and G. V. Chilingar, eds., Elsevier, New York, 328–331, 342–344.

Kreutzberger, M. E. and Peacor, D. R. (1988) Behavior of illite and chlorite during pressure solution of shaly limestone of the Kalkberg Formation, Catskill, New York: *J. Struct. Geol.* **10,** 803–811.

Lee, J. H., Ahn, J. H., and Peacor, D. R. (1985) Textures in layered silicates: Progressive changes through diagenesis and low-temperature metamorphism: *J. Sediment. Petrol.* **55,** 532–540.

Lee, J. H., Peacor, D. R., Lewis, D. D., and Wintsch, R. P. (1986) Evidence for syntectonic crystallization for the mudstone to slate transition at Lehigh Gap, Pennsylvania, U.S.A.: *J. Struct. Geol.* **8,** 767–780.

Levinson, A. A. (1955) Polymorphism among illites and hydrous micas: *Amer. Mineral.* **40,** 41–49.

Lonker, S. W. and Fitz Gerald, J. D. (1990) Formation of coexisting 1*M* and 2*M* polytypes in illite from an active hydrothermal system: *Amer. Mineral.* **75,** 1282–1289.

Maxwell, D. T. and Hower, J. (1967) High-grade diagenesis and low-grade metamorphism of illite in the Precambrian Belt series: *Amer. Mineral.* **52,** 843–857.

McKellar, I. C. (1966) Geological map of New Zealand, Sheet 25, Dunedin: Dept. Sci. Indust. Res., Wellington, New Zealand.

Merriman, R. J. and Roberts, B. (1985) A survey of white mica crystallinity and polytypes in pelitic rocks of Snowdonia and Llyn, North Wales: *Mineral. Mag.* **49,** 305–319.

Merriman, R. J., Roberts, B., and Peacor, D. R. (1990) A transmission electron microscope study of white mica crystallite size distribution in a mudstone to slate transitional

https://doi.org/10.1346/CCMN.1991.0390509 Published online by Cambridge University Press

sequence, North Wales, UK: *Contrib. Mineral. Petrol.* **106,** 27–40.

Morse, J. W. and Casey, W. H. (1988) Ostwald processes and mineral paragenesis in sediments: *Amer. Jour. Sci.* **288,** 537–560.

Mukhamet-Galeyev, A. P., Pokrovskiy, V. A., Zotov, A. V., Ivanov, I. P., and Samotoin, N. (1985) Kinetics and mechanism of hydrothermal crystallization of $2M_1$ muscovite: An experimental study: *Internat. Geol. Rev.* **27,** 1352–1364.

Odom, I. E. (1984) Glauconite and celadonite minerals: in *Micas, Reviews in Mineralogy, Vol. 13,* S. W. Bailey, ed., Mineralogical Society of America, Washington, D.C., 545–572.

Pandey, D., Baronnet, A., and Krishna, P. (1982) Influence of stacking faults on spiral growth of polytype structures in mica: *Phys. Chem. Minerals* **5,** 268–278.

Reynolds, R. C., Jr. (1963) Potassium-rubidium ratios and polymorphism in illites and microclines from the clay size fractions of proterozoic carbonate rocks: *Geochim. Cosmochim. Acta* **27,** 1097–1112.

Smith, J. V. and Yoder, H. S. (1956) Experimental and theoretical study of the mica polymorphs: *Mineral. Mag.* **31,** 209–231.

Środoń, J., Morgan, D. J., Eslinger, E. V., Eberl, D. D., and Karlinger, M. R. (1986) Chemistry of illite/smectite and end-member illite: *Clays & Clay Minerals* **34,** 368–378.

Velde, B. (1965) Experimental determination of muscovite polymorph stabilities: *Amer. Mineral.* **50,** 436–449.

Velde, B. and Hower, J. (1963) Petrological significance of illite polymorphism in Paleozoic sedimentary rocks: *Amer. Mineral.* **48,** 1239–1254.

Walker, J. R. and Thompson, G. R. (1990) Structural variations in chlorite and illite in a diagenetic sequence from the Imperial Valley, California: *Clays & Clay Minerals* **38,** 315–321.

Wintsch, R. P. (1978) A chemical approach to the preferred orientation of mica: *Bull. Geol. Soc. Amer.* **89,** 1715–1718.

Yau, Y. C., Peacor, D. R., and McDowell, S. D. (1987a) Smectite-to-illite reactions in Salton Sea shales: A transmission and analytical electron microscopy study: *J. Sediment. Petrol.* **57,** 335–342.

Yau, Y. C., Peacor, D. R., Beans, R. E., Essene, E. J., Lee, H. J., Kuo, L. C., and Cosca, M. A. (1987b) Hydrothermal experiments on candidate packing materials of smectite, illite and basalt: *Clays & Clay Minerals* **35,** 241–250.

Yau, Y. C., Peacor, D. R., Beans, R. E., Essene, E. J., and McDowell, S. D. (1988) Microstructures, formation mechanisms, and depth-zoning of phyllosilicates in geothermally altered shales, Salton Sea, California: *Clays & Clay Minerals* **36,** 1–10.

Yoder, H. S. and Eugster, H. P. (1955) Synthetic and natural muscovites: *Geochim. Cosmochim. Acta* **8,** 225–280.

(Received 4 November 1989; accepted 23 July 1991; Ms. 1960)

https://doi.org/10.1346/CCMN.1991.0390509 Published online by Cambridge University Press